Evaluation of Applying Retaining Shield Rotor for High-Speed Interior Permanent Magnet Motors

Jiancheng Zhang, Xiaoyan Huang, Youtong Fang, Wenping Cao

College of Electrical Engineering, Zhejiang University, Hangzhou 310027, China

This paper proposes a novel rotor structure for high-speed interior permanent magnet (IPM) motor to overcome the huge centrifugal forces under high-speed operation. Different from constructing by the conventional axial stack of silicon-steel laminations, the retaining shelf rotor is inter-sacked by high-strength stainless-steel plates to enhance the rotor strength to withstand the huge centrifugal forces. Both mechanical characteristics and electromagnetic behaviors of the retaining shelf rotor are analyzed using finite-element method (FEM) in this paper. Prototypes and experimental results are demonstrated to verify the design. The analysis and test results show that the proposed retaining shelf rotor designed could effectively enhance the rotor strength without sacrificing the electromagnetic performance, but some design constraints should be compromised.

Index Terms—Finite-element method (FEM), high-speed interior permanent magnet (IPM) motor, mechanical analysis, retaining shelf rotor.

I. INTRODUCTION

PERMANENT MAGNET (PM) MOTORS are widely used in many applications due to the well-known advantages of high power density, efficiency and power factor. In some applications such as electric vehicle traction motor, high-speed compressor motor and actuation motor in more-electrical aircraft, these motors are usually designed to be high-speed motors to have compact structure, which brings a challenge on rotor topology design.

Some techniques have been proposed to strengthen PM rotors [1]-[8]. For surface-mounted permanent magnet (SPM) motor, one of the most popular methods is to retain the magnets or rotor by a shrunk-on metallic shell or a fiber wrap, also called retaining sleeve [1]-[4]. The retaining sleeve needs to be carefully designed to avoid mechanical failure [3], [4]. Moreover, if the adding sleeve is made of conductive material, eddy currents will be induced, causing more rotor losses [1], [2]. Besides, the retaining sleeve increases the equivalent length of air gap, degrading the electromagnetic performances, which need to be compensated by increasing the amount of PM [5].

For interior permanent magnet (IPM) motor, the IPM rotor was often considered to have better mechanical properties, because the PMs are embedded and protected by rotor iron. But the actual situation is much more complicated. In order to reduce the leakage flux, there always exists a iron bridge adjacent to the PM, which makes the rotor design more complex. It is in a compromise between mechanical properties and electromagnetic performances, i.e., the wide bridge is good for rotor robust, but will degrade the electromagnetic performances due to the large amount of flux leakage; while, the thin bridge will result in less leakage flux, but maybe not strong enough to withstand the centrifugal forces at high speed [4]-[7]. And even in some cases, the retaining sleeve is still needed for IPM rotor [8].

In this paper, a novel rotor structure, called retaining shelf rotor, for high-speed interior permanent magnet (IPM) motor is proposed as shown in Fig. 1. Different from constructing by the traditional lamination stack of silicon-steel sheets, the novel rotor is inter-sacked by stainless-steel plates to enhance the mechanical strength, in which the stainless steel has much better mechanical properties especially in tensile yield strength to withstand the huge centrifugal forces. It needs to be stressed that the corresponding cavities for PMs exist both in silicon-steel sheets and stainless-steel plates as shown in Fig. 2, so the equivalent axial length of IPM motor will not be reduced.

In this paper, mechanical design characteristics and electromagnetic behaviors are analyzed to confirm the feasibility and superiority of applying retaining shelf rotor. The finite-element method (FEM) is adopted in both mechanical analysis and electromagnetic analysis. Then, the prototypes are manufactured to verify the analysis results and further validate the practicability of the design concept.
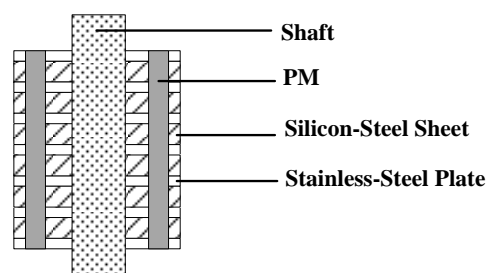

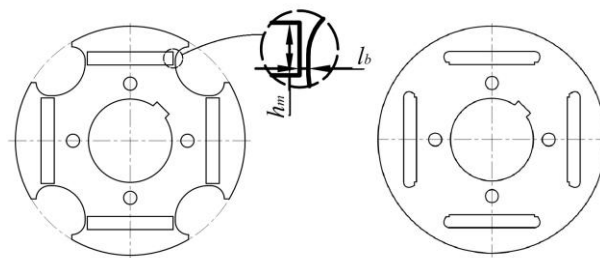Fig. 1. Configuration of IPM retaining shelf rotor.

Fig. 2. Configuration of silicon-steel sheet (left) and stainless-steel plate (right).

II. MECHANICAL ANALYSIS OF RETAINING SHELF ROTOR

A. Structure Force Analysis in Theory

The structure force analysis of retaining shelf rotor at high speed rotation is mainly focus on the interaction of silicon-steel sheets, stainless-steel plates and PMs. For simplifying the analysis problem, some assumptions are adopted as follows: 1) steady-state speed conditions only, 2) centrifugal forces dominant and 3) contact forces between silicon-steel sheets and stainless-steel plates neglected. In addition, under burst speed condition, the silicon-steel sheets have a lager deformation than stainless-steel plates, so the centrifugal forces of PMs will totally act on the stainless-steel plates.

Therefore, based on the assumptions and analysis above, the coupled multi-object 3D structure analysis model can be decoupled into two independent sub-models of 1) silicon-steel sheet under the only action of itself centrifugal force and 2) stainless-steel plate under both actions of itself and PMs' centrifugal forces. In general, compared to conventional rotor, the retaining shelf rotor improves the rotor burst speed by relieve the PMs' centrifugal forces from silicon-steel sheets.

B. Structure Stress Analysis in FEM

In this section, three different prototype rotors (Model-1, Model-2, Model-1+) including two conventional rotors and one retaining shelf rotor are constructed to analyze the mechanical performance of retaining shelf rotor in comparison. The specifications of the prototype high-speed permanent magnet rotor including the mechanical parameters of the materials are given in Table I. Table II shows the variable parameters for three rotors including width of magnetic bridges (l_b), thickness of PMs (h_m) and axial length (L) along with the corresponding burst speeds (V_{lim}) and magnetic flux per phase per pole (Φ), in which V_{lim} is analyzed by FEM and Φ is calculated by 3D electromagnetic FEM. The corresponding critical stress distributions of silicon-steel sheets and stainless-steel plates are shown in Figs. 3-4.

TABLE I
SPECIFICATIONS OF IPM ROTOR AND MATERIALS

Rotor outer diameter	104.4 mm	
Stack length	100 mm	
Maximum speed	20000 r/min	
PM	NdFeB 38UH	
Density	7.6g/cm3	
Steel type	Silicon steel	Austenitic stainless steel
Density	7.65g/cm3	7.83g/cm3
Young's modulus	200GPa	195GPa
Poisson's ratio	0.31	0.3
Tensile yield stress	410MPa	980MPa
Permeability	B-H curve	< 1.008

Model-1 is the initial design of a conventional rotor with traditional lamination stack of silicon-steel sheets. The retaining shelf rotor topology is adopted in Model-2, in which the configuration parameters of silicon-steel sheets keep same with Model-1. The burst speed of silicon-steel sheets without PMs, definitely higher than Model-1's, is designed as the burst speed of retaining shelf rotor. Thus, the axial length of stainless-steel plates which subjected with the total PMs'

centrifugal forces is determined by this burst speed. While in Model-1+, the configuration parameters of silicon-steel sheets are adjusted to reach the same critical rotation speed to Model-2. At the meantime, Φ should be designed similar to Model-2.

The analysis results demonstrate that the retaining shelf rotor increases 17.4% burst speed compared to the conventional rotor in this case. However, by adjusting the configuration parameters of silicon-steel sheets to achieve the same improvement of burst speed, it will cost 33% more PM material. In addition, in some cases such as high power density traction motor, the magnetic structures of IPM rotors are extremely compact and difficult for further adjustment and optimization. So in order to make the rotor suitable for high-speed operation, the retaining shelf rotor will be a good choice in such applications.

TABLE II
ROTOR CONFIGURATION PARAMETERS AND ANALYSIS RESULTS

		h_m/mm	l_b/mm	L/mm	V_{lim}/rpm	Φ/wb
Model-1	Si*	6	1	100	17571	0.01397
Model-2	Si*	6	1	83	20626	0.01388
	Au**	6	/	17		
Model-1+	Si*	8	1.5	100	20626	0.01402

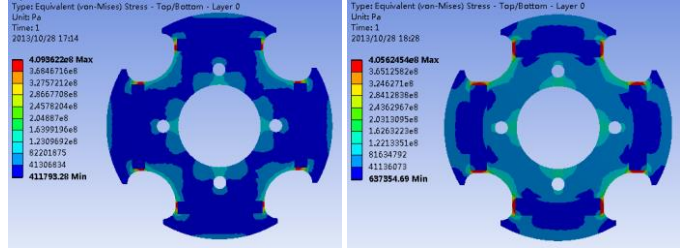Si*: silicon-steel sheets. Au**: stainless-steel plates.

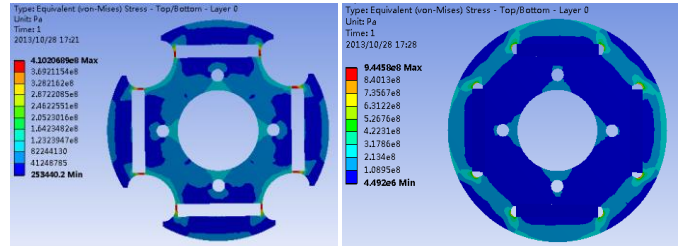Fig. 3. Stress distribution of silicon-steel plates in Model-1 and Model-1+.

Fig. 4. Stress distribution of silicon-steel and stainless-steel plates in Model-2.

C. Experiment Evaluation

The conventional rotor and the retaining shelf rotor are manufactured and assembled into one rotor prototype as shown in Fig. 5. The rotor configuration parameters are given in Table III. The axial length proportion of stainless-steel plates is set higher than Model-2 intentionally, so that the rotor burst over high speed must be caused by the stress failure of silicon-steel sheets. The test results of respective burst speed are recorded in Table III, and the rotor burst states over these burst speeds are shown in Fig. 6. The differences between test results and analysis results are 4.1% and 7.1%, in which the retaining shelf rotor has a better mechanical behavior in test.

So it could be concluded that the retaining shelf rotor can effectively improve the mechanical strength.

TABLE III
ROTOR CONFIGURATION PARAMETERS AND EXPERIMENT RESULTS

		h_m/mm	l_b/mm	L/mm	V_{lim}/rpm
Model-1	Si*	6	1	17	18321
Model-4	Si*	6	1	12	22206
	Au**	6	/	5	

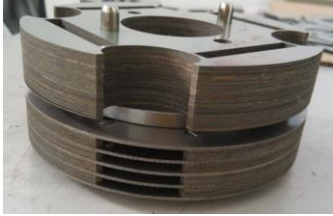Si*: silicon-steel sheets. Au**: stainless-steel plates.

Fig. 5. Test rotor assembly.

Fig. 6. Test rotor burst state over 18321 rpm (left) and 22206 rpm (right).

TABLE IV
SPECIFICATIONS OF IPMSMS IN DESIGN AND PROTOTYPE

	Design	Prototype
Stator outer diameter	155 mm	
Rotor outer diameter	104.4 mm	
Air-gap length	0.8 mm	
Stack length	100 mm	
Slot number	36	
Rated power	1.5 kW	
Rated current	2.5 A	
Number of turns per phase	2	24
Number of strands per coil	12	1
Rated speed	18,000 r/min	1,500 r/min

III. ELECTROMAGNETIC ANALYSIS OF RETAINING SHELF ROTOR MOTOR

When applying the retaining shelf rotor, there will be doubt as to whether this novel rotor influences the electromagnetic behaviors of IPM motor. So in this section, the effects of replacing a proportion of silicon-steel sheets by stainless-steel plates on the electromagnetic properties of IPM motor are discussed. A 4-pole 3-phase interior permanent magnet synchronous motor (IPMSM) with rating of 1.5kW @18,000rpm is designed and prototyped for study. But limited to the laboratory test conditions, the manufactured prototype is tested under 1,500rpm after adjusting the winding design. The specifications of the IPMSMs both in design and prototype are given in Table IV.

A. Modeling for Electromagnetic Finite Element Analysis

Because of the complex rotor topology, the 3D finite element model is necessary to analyze electromagnetic behaviors of the IPMSM with retaining shelf rotor. In order to simplify the 3D model and save calculation time, considering the end effects, the rotation cyclic boundary condition and axial symmetry boundary condition are used, so that it is sufficient to analyze the finite element model with a quarter model in circumference and a half in axial as shown in Fig. 7.
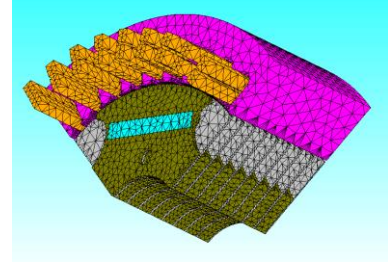

Fig. 7. Finite element model.

B. FEM Analysis and Discussion

1) No-load back-EMF: It is the prominent characteristic of PM motor, which can verify the magnetic design of the motor. In order to reveal the effects of the retaining shelf rotor, five model cases with different axial length proportions of stainless-steel plates are analyzed, they are Model-1: all silicon-steel, Model-2: 1/6 is stainless-steel, Model-3: 1/5 is stainless-steel, Model-4: 1/4 is stainless-steel, Model-5: 1/3 is stainless-steel. The FEM analysis results of no-load back-EMF waveforms are shown in Fig. 8. Results indicate that the amplitude of fundamental back-EMF is decreasing along with the increase of stainless-steel proportion. But the decreasing amplitude is small with 3.6% maximum and 1.6% minimum.
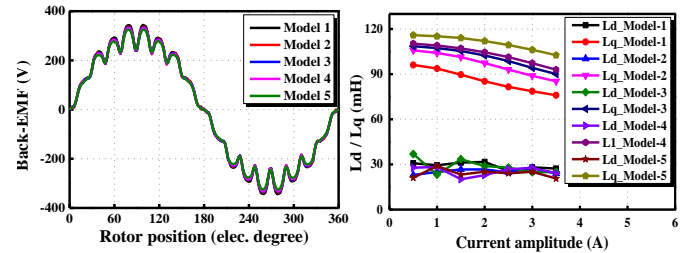

Fig. 8. Comparison of back-EMF waveforms and L_d, L_q.

2) Inductances of L_d and L_q: They are the key parameters of IPMSM which directly influence the performances of torque output and flux-weakening control. Because the inductances are affected by magnetic saturation, so the inductance variations against input current under maximum torque per ampere (MTPA) condition are analyzed. The results shown in Fig. 8 indicate that L_q is decreasing along with the increase of stainless-steel proportion with the decreasing amplitude of 5% ~ 25%, whilst the L_d is almost unaffected.

3) Torque performance: The torque waveforms of five models at rated current under MTPA condition are presented in Fig. 9. The results show that in this case the torque performance such as average torque is almost not affected at all with maximum decreasing amplitude of 3%. Even so, we

should realize that the ratio of reluctance torque to total torque in this case is less than 10%, thus the theoretically estimated torque decline is more or less 2%. Therefore, the higher the ratio of reluctance torque in IPM motors is, the retaining shelf rotor affects the torque performance more severely.
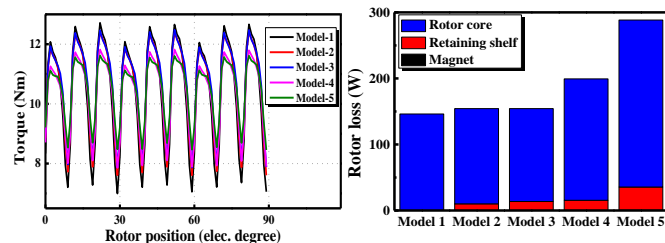

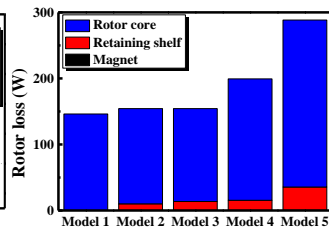Fig. 9. Comparison of torque waveforms.   Fig. 10. Iron loss @2.5A rms.

4) Rotor Iron Loss: The magnetic field in rotor is changed when applying retaining shelf rotor. The eddy current effects in rotor of magnets, retaining shelf and rotor yoke are analyzed. The iron losses in rotor are calculated at rated condition using 3D time-stepping FEM. The results are shown in Fig. 10. It is shown that the rotor loss nearly won't be affected when the axial length proportions of stainless-steel plates are less than 1/5; whilst the axial length proportions of stainless-steel plates are more than 1/4, the rotor loss will increase dramatically. This exponential increase results from the exponential increase of iron loss in the silicon steel, where the magnetic density is increased due to the high proportion of stainless steel.

C. Experiment Evaluation

The prototypes of IPMSMs with conventional rotor and retaining shelf rotor (Model-4) are shown in Fig. 11. The comparisons of measured phase back-EMF waveforms and measured torque with current of 2.5A are presented in Fig. 12. Table V shows the measured Inductances of L_d and L_q with no load. In general, the test results show good agreements with FEM results.

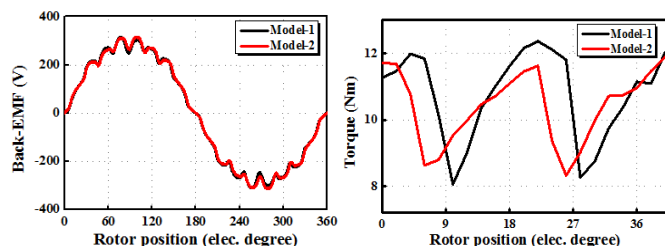Fig. 11. Prototypes of conventional rotor (left) and retaining shelf rotor (right).

Fig. 12. Test reults of back-EMF waveforms and torque waveforms.

	L_d/mH	L_q/mH
Conventional rotor	39.35	90.29
Retaining shelf rotor	34.04	75.53

IV. CONCLUSION

The retaining shelf rotor has been proved to be an effective approach to improve the mechanical strength of IPM rotor in this paper. In order to maximize its strengths whilst minimizing its weaknesses, the following design constraints should be compromised when using the retaining shelf rotor approach. On the one hand, pole shoes or the iron area peripheral to the magnetic bridge need to be designed narrow to increase the burst speed. But on the other hand, the negative effects of the increased axial proportions of stainless-steel plates on torque and rotor losses should be well considered.

REFERENCES

[1] Bianchi Nicola, Bolognani Silverio, Luise Fabio, "Potentials and Limits of High-Speed PM Motors," *IEEE Trans. Ind. Appl.*, vol. 40, no. 6, pp. 1570-1578, 2004.
[2] Zhou Fengzheng, Jianxin Shen, Weizhong Fei, Ruiguang Lin, "Study of Retaining Sleeve and Conducticve Shield and Theri Influence on Rotor Loss in High-Speed PM BLDC Motors," *IEEE Trans. Magn.*, vol. 42, no. 10, pp. 3398-3400, October 2006.
[3] Smith D.J.B., Mecrow B.C., Atkinson G.J., Jack A.G., Mehna A.A.A., "Shear Stress Concentrations in Permanent Magnet Rotor Sleeves," *Electrical Machines (ICEM), 2010 XIX International Conference on*, pp. 1-6, 2010.
[4] Binder Andreas, Schneider Tobias, Klohr Markus, "Fixation of buried and surface-mounted magnets in high-speed permanenrt-magnet synchronous motors," *IEEE Trans. Ind. Appl.*, vol. 42, no. 4, pp. 2843-2848, July/August 2006.
[5] Sung-Il Kim, Young-Kyoun Kim, Geun-Ho Lee, Jung-Pyo Hong, "A Novel Rotor Configuration and Experimental Verificaion of Interior PM Synchronous Motor for High-Speed Applications," *IEEE Trans. Magn.*, vol. 48, no. 2, pp. 843-846, February 2012.
[6] Jung Jae-Woo, Lee, Byeong-Hwa Hwa, Kim Do-Jin, Hong Jung-Pyo Pyo, Kim Jae-Young, Jeon Seong-Min, Song Do-Hoon, "Mechanical Stress Reduction of Rotor Core of Interior Permanent Magnet Synchronous Motor," *IEEE Trans. Magn.*, vol. 48, no. 2, pp. 911-914, February 2012.
[7] Lovelace E.C., Jahns T.M., Keim T.A., Lang Jeffrey H., "Mechanical design considerations for conventionally laminated, high-speed, interior PM synchronous machine rotors," *IEEE Trans. Ind. Appl.*, vol. 40, no. 3, pp. 806-812, February 2012.
[8] Jannot X., Vannier J.-C., Marchand C., Gabsi M., Saint-Michel J., Sadarnac D., "Multiphysic Modeling of a High-Speed Interior Permanent-Magnet Synchronous Machine for a Multiobjective Optimal Design," *IEEE Trans. Energy. Convers.*, vol. 26, no. 2, pp. 457-467, June 2011.